Syst. Biol. 64(2):215–232, 2015

DOI:10.1093/sysbio/syu088
Advance Access publication November 13, 2014

Integrating Fossils, Phylogenies, and Niche Models into Biogeography to Reveal Ancient Evolutionary History: The Case of *Hypericum* (Hypericaceae)

ANDREA S. MESEGUER[1,2,*], JORGE M. LOBO[3], RICHARD REE[4], DAVID J. BEERLING[5], AND ISABEL SANMARTÍN[1]

[1]*Department of Biodiversity and Conservation, Real Jardín Botánico, CSIC, Plaza de Murillo 2, 28014 Madrid, Spain;* [2]*INRA, UMR 1062 CBGP Campus International de Baillarguet, 34988 Montferrier-sur-Lez, France;* [3]*Department of Biogeography and Global Change, Museo Nacional Ciencias Naturales-CSIC, 28006 Madrid, Spain;* [4]*Department of Botany, Field Museum of Natural History, Chicago, IL 60605, USA and* [5]*Department of Animal and Plant Sciences, University of Sheffield, Sheffield S10 2TN, UK*

**Correspondence to be sent to: Department of Biodiversity and Conservation, Real Jardín Botánico, CSIC, Plaza de Murillo 2, 28014 Madrid, Spain; E-mail: asanchezmeseguer@gmail.com and isanmartin@rjb.csic.es*

Received 31 January 2014; reviews returned 27 May 2014; accepted 7 November 2014
Associate Editor: Austin Mast

Abstract.—In disciplines such as macroevolution that are not amenable to experimentation, scientists usually rely on current observations to test hypotheses about historical events, assuming that "the present is the key to the past." Biogeographers, for example, used this assumption to reconstruct ancestral ranges from the distribution of extant species. Yet, under scenarios of high extinction rates, the biodiversity we observe today might not be representative of the historical diversity and this could result in incorrect biogeographic reconstructions. Here, we introduce a new approach to incorporate into biogeographic inference the temporal, spatial, and environmental information provided by the fossil record, as a direct evidence of the extinct biodiversity fraction. First, inferences of ancestral ranges for those nodes in the phylogeny calibrated with the fossil record are constrained to include the geographic distribution of the fossil. Second, we use fossil distribution and past climate data to reconstruct the climatic preferences and potential distribution of ancestral lineages over time, and use this information to build a biogeographic model that takes into account "ecological connectivity" through time. To show the power of this approach, we reconstruct the biogeographic history of the large angiosperm genus *Hypericum*, which has a fossil record extending back to the Early Cenozoic. Unlike previous reconstructions based on extant species distributions, our results reveal that *Hypericum* stem lineages were already distributed in the Holarctic before diversification of its crown-group, and that the geographic distribution of the genus has been relatively stable throughout the climatic oscillations of the Cenozoic. Geographical movement was mediated by the existence of climatic corridors, like Beringia, whereas the equatorial tropical belt acted as a climatic barrier, preventing *Hypericum* lineages to reach the southern temperate regions. Our study shows that an integrative approach to historical biogeography—that combines sources of evidence as diverse as paleontology, ecology, and phylogenetics—could help us obtain more accurate reconstructions of ancient evolutionary history. It also reveals the confounding effect different rates of extinction across regions have in biogeography, sometimes leading to ancestral areas being erroneously inferred as recent colonization events. [Biogeography; Cenozoic climate change; environmental niche modeling; extinction; fossils; *Hypericum*; phylogenetics.]

In historical biological disciplines such as macroevolution or macroecology, which are not in general amenable to experimentation, scientists need to rely on present-day observations to make inferences about the past. For example, systematists use current variation in morphological and/or DNA traits to reconstruct phylogenetic relationships and rates of nucleotide mutation. In historical biogeography, biogeographers use phylogenetic relationships and present distribution data to infer ancestral geographic ranges and past biogeographic events (Lomolino et al. 2010). Assuming that "the present is the key to the past" (and the future) is to a certain extent inevitable in a comparative observational science that deals with scales of space and time at which experimental manipulation is hardly possible (Lomolino et al. 2010). This assumption permeates methods in biogeographic inference. For example, it is the basis for the assignment of cost values in event-based biogeographic methods, in which processes such dispersal and extinction are penalized (higher cost) because they partly erase previous distributional history—preventing the recovery of "phylogenetically conserved" distribution patterns—, whereas vicariance and within-area speciation are given a low cost because they involve inheritance of distributional ranges (Ronquist and Sanmartín 2011). Similarly, in parametric methods such as dispersal–extinction–cladogenesis (DEC), ancestral ranges are inferred conditional on the distribution of the extant descendants; however, correct estimates can only be obtained if extinction and dispersal rates—which are modeled as stochastic processes evolving along branches—are low in relation to cladogenesis (Ree and Smith 2008).

One scenario that is particularly damaging to the assumption that the present is the key to the past is when extinction rates are so high that the biodiversity we observe today is no longer representative of the historical diversity. Extinction erases the evidence of past speciation events and, as we move back into the past, there is less information to infer ancestral states. This results in inferences for basal cladogenetic events that are often uncertain and tend to include a large number of areas (Ronquist and Sanmartín 2011), or even wrong biogeographic reconstructions if extinction has been particularly high within an area (Lieberman 2005). A possible solution comes from the fossil record, which provides direct evidence on the extinct biodiversity fraction that we cannot observe. So far, the use of fossils in biogeography has been limited to the provision of calibration points for phylogenetic dating

(Ho and Phillips 2009). However, recent biogeographic studies have shown that incorporating the geographic distribution of fossils to the analysis may change dramatically the inferred biogeographic scenario (Mao et al. 2012; Nauheimer et al. 2012; Wood et al. 2012). These studies, however, have relied on using fossils as additional lineages in the phylogeny, which requires coding the morphological traits of the fossil taxa alongside the extant molecular characters (e.g., Mao et al. 2012), or assuming arbitrary branch lengths for the fossil lineage (Nauheimer et al. 2012).

In addition to the temporal and spatial aspect, fossils can provide information on the climatic preferences of ancestral lineages, that is, the environmental conditions in which they reproduced and maintained viable populations, which may then be used to reconstruct past geographic ranges (Sanmartín 2012; Stigall 2012). Surprisingly, biogeographers have been slow to incorporate ecological information to their biogeographic models. For example, it has become common practice in parametric biogeography to include information on the past configuration of areas in the time-dependent transition matrix that governs the movement between geographic states (Buerki et al. 2011; Mao et al. 2012). Dispersal rates are scaled to reflect the presence of a temporal land bridge, increasing the probability of movement between two regions (e.g., the Beringian Bridge between Asia and North America). However, land dispersal is probably as much conditioned by the presence of a physical bridge as by the existence of climatic conditions along the bridge that are within the ecological limits of the dispersing organism (Sanmartín et al. 2001; Wiens and Donoghue 2004). For example, limiting climatic tolerances might be behind some global biodiversity patterns such as the Latitudinal Diversity Gradient: the excess of plant species in tropical regions compared with temperate latitudes has been explained by the greater climatic stability of these regions over time, and the inability of many lineages that originated in tropical conditions to evolve the relevant adaptations required to move into the seasonal temperate climates (Wiens and Donoghue 2004; Donoghue 2008).

Environmental niche modeling (ENM) techniques in combination with phylogenetic evidence offer one way to approximate the climatic preferences of lineages and thus identify potential evolutionary changes in climatic tolerances or detect areas that were climatically adequate in the past (e.g., Yesson and Culham 2006; Smith and Donoghue 2010). These studies, however, are limited by the fact that they are based exclusively on present-day distributions and assume to some extent that ancestral lineages shared the same climatic requirements as their extant descendants. Although this might be true for short time scales, it becomes less likely over geological time scales of millions of years (Peterson 2011; Stigall 2012). To break this assumption, some paleoecologists have used ENM models based on fossil distributions to trace the evolution of climatic preferences over longer time scales (Stigall Rode and Lieberman 2005; Stigall 2012). But the incompleteness of the fossil record and the lack of environmental data in the deep past have so far limited this approach to recent geological periods (Nogués-Bravo et al. 2008) and small geographical regions (Maguire and Stigall 2009).

Here, we introduce a new approach to incorporate into biogeographic inference the temporal, spatial, and climatic information provided by the fossil record as direct evidence of the extinct biodiversity fraction. First, the spatial range of a fossil is used to constrain the inference of ancestral areas for the node to which that fossil is assigned, thus obviating the need to include it as an additional lineage in the phylogenetic analysis. Second, we use ENM techniques based on fossil and extant distribution data and new global-scale bioclimatic models that extend into the early Cenozoic (Beerling et al. 2009, 2011, 2012; Bradshaw et al. 2012) to reconstruct the climatic preferences and potential distribution of ancestral lineages over time. Finally, we use the climatic and spatial information provided by fossils to build a biogeographic model that takes into account "ecological" connectivity through time in order to detect regions that were in the past within the lineage's climatic tolerances and might have acted as dispersal corridors, or which lacked suitable habitat and might have acted as climatic barriers or have been subjected to local extinction.

To show the potential of our approach, we used the angiosperm plant genus *Hypericum* L. ("St. John's wort," Hypericaceae). This genus, one of the 100 largest among angiosperms (ca. 500 species), has a worldwide distribution and a fossil record that extends back to the Early Cenozoic (Fig. 1a,b; Meseguer and Sanmartín 2012). A recent study (Meseguer et al. 2013) reconstructed *Hypericum* ancestors as Early Cenozoic plants that migrated from Africa into the Western Palearctic at a time when tropical climates dominated northern latitudes, and later from the Western Palearctic to other Holarctic regions while presumably developing adaptations to colder climates, such as the herbaceous habit or unspecialized corollas. Their reconstruction, however, was based only on extant taxa, and it is at odds with the *Hypericum* fossil record. The oldest fossil representative, *Hypericum antiquum*, is from northern Asia (Fig. 1c; Meseguer and Sanmartín 2012), a region that is marginally represented across extant lineages but which harbors many described fossil species (Fig. 1b) and had a warmer climate in the past (Tiffney 1985a). Meseguer et al. (2013) suggested that the disagreement between the fossil record and their biogeographic reconstruction might be explained by climate cooling and high extinction rates in Asia during the Neogene, which would have removed many early divergent lineages in this region. In this study, we test this hypothesis by reconstructing the spatio-temporal evolution of *Hypericum* using a fossil-informed approach to ENM and biogeographic reconstruction that integrates different lines of evidence (i.e., historical

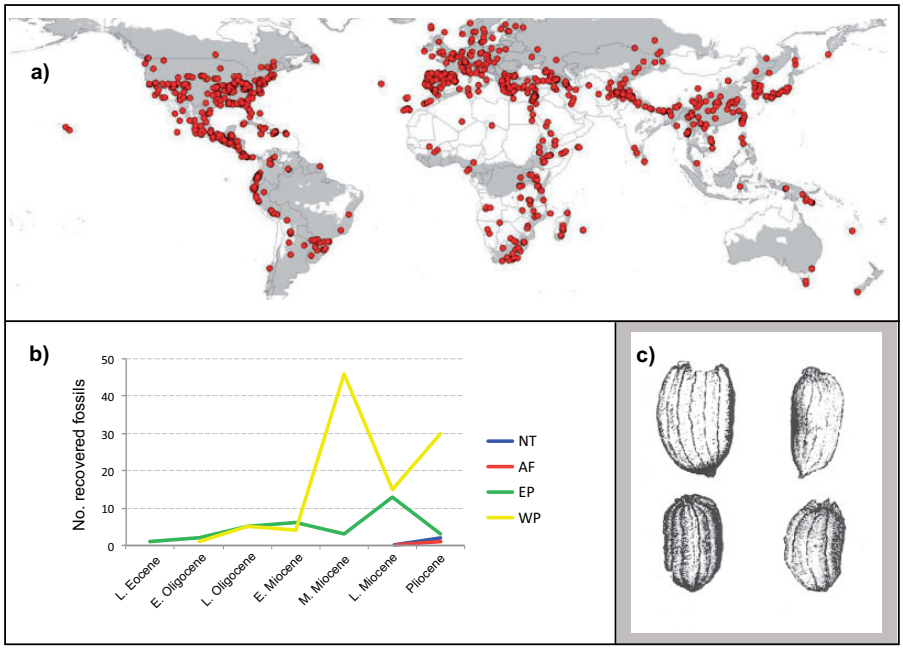

FIGURE 1. a) Potential distribution of *Hypericum* in the present (in grey); the map was created by projecting the climatic tolerances of extant *Hypericum* species based on 1033 occurrences (red dots) over present climatic conditions. b) Number of fossil remains of *Hypericum* through time and across biogeographic regions. Line colors correspond with the discrete areas defined in the inset map of Figure 4. c) Fossil seeds of *Hypericum antiquum* Balueva & Nikitin, 4 seeds, × 33 (reproduced with permission from Arbuzova 2005). Color version of this figure is available at *Systematic Biology* online.

and ecological, extinct and extant). The ancient origin of *Hypericum*, global geographic distribution and high levels of species diversity constitute a new challenge for fossil-modeling ENM studies, focused so far on individual species with restricted ranges.

METHODS

Hypericum Fossil Record and Assignment to Phylogenetic Clades

Hypericum has a rich fossil record that extends from the Late Eocene to present times (Fig. 1b; Supplementary Table S1 in online Appendix 1, available at http://dx.doi.org/10.5061/dryad.5845b). This record comprises some macrofossils (leaves), but mostly consists of microfossil remains, seeds and pollen. Among them, seeds are particularly distinctive in *Hypericum*. The typical seeds in the family Hypericaceae are small, narrowly cylindrical to ovoid-cylindrical, or ellipsoid (Robson 1981), with a size ranging from 8 to 0.3 mm. They also present brownish to blackish tannin contents. According to Corner (1976), the shape of the exotegmen cells in Hypericaceae—tubular or radially elongated and with stellate-undulate or lobate facetes—is very characteristic of this family and found only in a few other families: Clusiaceae, Elatinaceae, and Geraniaceae. In addition, Hypericaceae (excluding *Psorospermum* with fleshy tegmen cells) and Clusiaceae seeds have a unique structure with large, lignified and tabular, thick-walled stellate cells in the exotegmen. Hypericaceae seeds are distinguishable from Clusiaceae seeds in that the former are generally smaller and do not present an aril.

Hypericum seeds can be distinguished from the seeds of other Hypericaceae genera by their small size (<1.5 mm). They also lack the cartilaginous wing present in the seeds of tribe Cratoxyleae, and the orange or black glands exhibited by some species of genera *Harungana* and *Vismia* from tribe Vismieae (Stevens 2007). Additionally, *Hypericum* seeds possess a particular wing venation, composition, and disposition of appendages that are not found in any other member of Hypericaceae. The wing is thin and papery and is sometimes reduced to a carina, basal prolongation, or apiculi (Robson 1981). The testa or outer layer presents different ornamentations or sculpture patterns that have been used to characterize entire taxonomical sections (Robson 1981); these range from reticulate to scaraliform, and to papillose (see table 2 in Meseguer and Sanmartín 2012). Although the reticulate pattern can be found in other Hypericaceae genera, the scaraliform and the papillose patterns are unique to *Hypericum* and can be used to assign fossil seeds to this genus (Meseguer and Sanmartín 2012).

The oldest fossil remains of the genus, the Late Eocene fossil seeds of *H. antiquum*, have been found in West Siberia (Arbuzova 2005, Fig. 1c). These fossil seeds share with genus *Hypericum* characteristics like their small size (0.4–0.65 × 0.25–0.35 mm), black color, and cylindrical shape (i.e., seeds are longitudinally slightly bent toward the raphe). Moreover, the presence of meridian ribs on the fossil seed testa resemble the "ribbed scalariform"

pattern present in various extant sections that are grouped into three distantly related clades in Meseguer et al. (2013)'s phylogeny: the early diverging section *Elodes* (Clade A), the New World sister-sections *Brathys* and *Trigynobrathys* (Clade B), and the Old World section *Drosocarpium* (Clade E). No additional characters in the seeds of these sections, though, allow us to assign the fossil to one of them. Magallón and Sanderson (2001, p. 1766) suggested that in the absence of explicit phylogenetic analyses including the fossil, the existence of synapomorphies could be used as an empirical criterion to determine the phylogenetic assignment of fossils. If a fossil presents the synapomorphies that characterize the extant members of a particular subclade within a larger clade, then this fossil can be assigned unambiguously to the crown group of the larger clade (e.g., *H. antiquum* displays the ribbed scaraliform sculpture pattern characteristic of the *Elodes* subclade within *Hypericum* so it can be identified as a crown group member of genus *Hypericum*). Conversely, if a fossil displays some, but not all the synapomorphies shared by extant members of a clade, then it is considered to be a stem lineage representative. Besides the scalariform seed testa, the fossil seeds of *H. antiquum* do not display any other particular feature (apomorphy) that distinguishes them from the seeds of other extant clades in *Hypericum*. Therefore, in here we chose to follow the conservative approach of Magallón and Sanderson (2001) and we assigned the fossil remains of *H. antiquum* to the crown node from which all living *Hypericum* are descendants, which is also the most recent common ancestor of the three clades exhibiting the scalariform seed testa, that is, clades A, B, and E in Meseguer et al. (2013).

The next oldest fossil remains are seeds of the fossil species *H. septestum*, from Lower Oligocene deposits again in the Eastern Palearctic (EP) region (Tomsk, Russia; Arbuzova 2005). This species became a common element in the Palearctic fossil record of the genus from the Late Oligocene to the Pliocene (Meseguer and Sanmartín 2012). Although characters such as the size, color, and disposition of the appendages identify these seeds as belonging to *Hypericum* (see above), the sculpturing pattern of the testa (i.e., reticulate) is the most common within *Hypericum* and it is also present in other Hypericaceae genera. Thus, these fossil seeds could not be assigned with confidence to any subclade within *Hypericum* based on this character, and we did not use them for node calibration in any subsequent dating or biogeographic analyses. The same applied to other Oligocene to Pliocene fossils such as *Hypericum tertiarium* Nikitin, *Hypericum miocenicum* Dorof. emend. Mai, or *Hypericum holyi* Friis, and to other remains that have been attributed to extant species of *Hypericum*, such as *Hypericum perforatum fossilis* or *Hypericum androsaemum fossilis* (Meseguer and Sanmartín 2012), which have also reticulate testa patterns. On the other hand, all these fossils were included in the ENM analysis, because the focus of this analysis was to model the climatic niche of genus *Hypericum* as a whole, not of each subclade independently.

Although most fossil remains described in *Hypericum* are seeds, fossil pollen has also been attributed to the genus. *Hypericum* pollen has a basic tricolporate plan, not particularly distinctive from other angiosperm lineages (Meseguer and Sanmartín 2012). Yet, several basic pollen types have been described, corresponding to major morphological sections (Clarke 1981), and *Hypericum* pollen grains have been successfully identified in ecological (Hedberg 1954) and forensic studies (Mildenhall 2006). Fossil pollen is generally considered less informative for biogeographic studies than macrofossil remains because pollen could be deposited a long distance away from the locality the plant inhabits, through wind, pollinators, or other dispersal vectors. Conversely, *Hypericum*, seeds are shed from the plant by the dehiscence of the capsule and generally fall near the parent plant. Although wind, water, or bird dispersal could occur incidentally in Hypericum, these seeds are probably not efficiently dispersed over long distances (Robson 1981). We therefore limited the use of fossil remains in our study to *Hypericum* seeds, with some exceptions: Oligocene and Miocene fossil pollen from Spain (Cavagnetto and Anadón 1996; Barrón et al. 2010) and Pliocene pollen occurrences from Colombia (van der Hammen 1974; Wijninga and Kuhry 1990) and Ethiopia (Bonnefille et al. 1987; see Supplementary Table S1). The reason for this is that: (i) these fossil pollen represent the only fossil record of *Hypericum* in Africa and South America; (ii) *Hypericum* pollen is generally dispersed by insects and occasionally by birds (Janeček et al. 2007), and therefore, it is expected to disperse over shorter distances than in anemophilous (wind-dispersed) plants; moreover, given the coarse resolution used in our ENM climate models (see below), it is unlikely that these fossil pollen grains come from a geographic region different from where they were assigned; (iii) the American Pliocene remains have been described from high altitude habitats in the Andes where *Hypericum* is currently a prominent component of the Paramo flora (Nürk et al. 2013b).

Distributional and Climatic Data

Distribution data for extant *Hypericum* species were obtained from taxonomic monographs (Robson 1981-onwards), herbarium collections (e.g., MA), and online databases (GBIF, http://www.gbif.org). Additionally, distribution data for species of *Triadenum* L., *Santomasia* N. Robson, and *Thornea* Breedlove & McClintock were included; these genera appear nested within *Hypericum* in most molecular studies (Ruhfel 2011; Meseguer et al. 2013; Nürk et al. 2013a). Distributions were georeferenced when latitudinal and longitudinal data were not provided and all data points were collated to exclude ambiguous occurrences (e.g., points in the sea or in regions where *Hypericum* has never been described). In total, 1033 occurrences were included, representing more than 160 identified species. Fossil distribution data (143 records; Supplementary Table S1 in online Appendix 1 available at http://dx.doi.org/10.5061/dryad.5845b.)

were obtained from the literature (Meseguer and Sanmartín 2012) and online resources (Paleobiology Database, http://paleodb.org/). We grouped non-Pleistocene fossil records into two time slices to ensure an adequate number of occurrences to model ancestral species data: "greenhouse" lineages covering the Eocene, Oligocene, and Early Miocene periods (68 records corresponding to 18 grid cells of 2.5°× 3.75°) and "coldhouse" fossil lineages, spanning the Late Miocene and Pliocene periods (65 records, 19 grid cells). The boundary between greenhouse and coldhouse time slices was set at the Late Miocene Cooling event (LMC, about 10 Ma), a dramatic drop in temperature following the Middle Miocene Climatic Optimum (Zachos et al. 2008). This is a period when important changes in vegetation occurred, including the replacement of the mixed-mesophytic forest by a boreal coniferous forest across the northern regions of Eurasia and North America (Schneck et al. 2012). Fossil paleocoordinates were calculated with the PointTracker application of the Paleomap software (Scotese 2010).

Climatic data for current conditions (≈1950–2000) were extracted from WorldClim (Hijmans et al. 2005). For past scenarios, we used six Hadley Centre-coupled ocean-atmosphere general circulation models (HadCM3L) that incorporate the effect of changes in atmospheric CO_2 concentration; the latter has been shown to be a good proxy for variations in global temperatures (Beerling and Royer 2011). These simulations were generated with the same underlying algorithms and the same set of variables (monthly temperature and precipitation values at a resolution of 2.5°× 3.75°), and represent major warming or cooling events in the Cenozoic: (i) an Early Eocene climate simulation with representation of Early Eocene (55 Ma) paleogeography (continental coastline and ice sheet configuration) and 1120 ppm CO_2 concentration to represent peak Eocene warmth; (ii) the same HadCM3L model set-up but with a lower CO_2 concentration of 560 ppm, to represent the drop in temperature at the Terminal Eocene Event (TEE); (iii) a 400 ppm CO_2 Late Miocene simulation representing the early warm period of the Miocene (Mid Miocene Climatic Optimum, 15 Ma); (iv) the same Miocene model set-up but with 280 ppm CO_2 concentration, representing the cold and dry conditions prevalent after the LMC event—details of the HadCM3L model set-up for the Eocene and the Miocene simulations are given in Beerling et al. (2011, 2012) and Bradshaw et al. (2012), respectively; (v) a 560 ppm CO_2 Pliocene simulation (Beerling et al. 2009) of the conditions at the Mid-Pliocene warming event (3.6–2.6 Ma); and (vi) a simulation of the Preindustrial World with 280 ppm CO_2 to provide a baseline HadCM3L climate before the industrial revolution from Beerling et al. (2012).

Environmental Niche Modeling

From WorldClim we selected the seven climatic variables that were used in the paleoclimate simulations (Beerling et al. 2012), which represent important vegetation predictors: annual precipitation, annual variation in precipitation, maximum monthly precipitation, maximum monthly temperature, mean annual temperature, minimum monthly precipitation, and minimum monthly temperature. Using these variables, we also estimated two bioclimatic indices: aridity and continentality, calculated following the formulas provided by Valencia-Barrera et al. (2002).

Since ENM results are highly dependent on the number and identity of the predictor variables (Beaumont et al. 2005), we firstly discriminated the most relevant climatic variables able to explain present *Hypericum* distribution using an ecological-niche factor analysis (ENFA; Hirzel et al. 2002; Calenge and Basille 2008) with the terrestrial world as the background area. This analysis is based on occurrences of extant species and the above-mentioned climatic variables, at a resolution of 10 arc-minutes (around 20 × 20 km). This procedure compares the climatic data of presence localities against the climatic conditions found throughout the study area, thereby computing uncorrelated factors that can explain both species marginality (the distance between the species optimum and the average climatic conditions in the study area) and specialization (the ratio between the climatic variability in study area and the variability associated with the focal species). Marginality thus represents the deviation of the niche space in the focus species from the global conditions available, while specialization would represent the breadth of the niche space of the species against those available in the study area. Factors were retained based on their eigenvalues relative to a broken-stick distribution (Hirzel et al. 2002). Predictor climatic variables selected were those showing the highest correlation values (factor scores >0.3) with the retained ENFA factors: annual precipitation, annual variation in precipitation, maximum and minimum monthly precipitation, minimum monthly temperature, aridity, and continentality. The low number of fossil occurrences prevents their use in separate ENFA analyses, so we assumed that the selected climatic variables were those with the higher explanatory capacity for all time periods analyzed.

To model the potential distribution of *Hypericum* in the past, we estimated maximum and minimum values for the above-selected climatic variables considering the distribution localities of present, greenhouse and coldhouse fossil lineages, transferring these conditions to the geographical space by using a generalized intersection procedure (Jiménez-Valverde et al. 2011). This simple method based on geometrical set theory was preferred over more complex modeling techniques based on the statistical fitting of data or machine-learning procedures capable of capturing complex spatial patterns, such as MaxEnt (Phillips et al. 2006), because it requires only "presence" data and is thus more appropriate for the often spatially biased fossil record (Jiménez-Valverde et al. 2011; Varela et al. 2011). Both statistical and machine-learning techniques require

pseudo or background absences generally selected at random from the whole distribution area, a risky procedure in the case of ENM models based on fossil data. The incompleteness of the fossil record connotes that occupancy probabilities can be biased by the unequal density of observations used in the analysis: some areas might simply have preserved more fossil data than others (Aarts et al. 2011; Hastie and Fithian 2013). In all cases, both current and paleocoordinates were resampled to a resolution similar to the one used in the paleomaps (2.50°× 3.75°). Specifically, we projected the climatic range from: (i) present-day occurrences based on extant data over present climatic world conditions, (ii) "coldhouse" fossil occurrences over the Late Miocene and Pliocene climatic simulations, and (iii) "greenhouse" fossil occurrences onto the Early Eocene, Late Eocene, and Early Miocene past climatic simulations, respectively. These models allowed us to identify areas in the underlying paleo-continental reconstruction (Markwick 2007) with suitable climate for *Hypericum* during the relevant paleotime frame using the available occurrences of each period. These binary representations were transformed into continuous ones by calculating the scale-invariant Mahalanobis distance (MD) from the average climatic conditions representing the lineage's hypothetical "climatic optimum" (Varela et al. 2011). We also examined the changes through time in the geographic area with favorable conditions for *Hypericum* across biogeographic regions (as defined in the biogeographic analysis) by dividing the MD scores into quartiles (from Q1 to Q4). Finally, to test the sensitivity of our analyses to the boundary selected between the greenhouse and coldhouse time slices, especially in relation to the variable Miocene period (Zachos et al. 2008), we repeated all the analyses after removing all Miocene records.

Phylogenetic and Lineage Divergence Estimation

To reconstruct ancestral geographic ranges and biogeographic events in *Hypericum*, we used the chloroplast data set of Meseguer et al. (2013), which is based on three chloroplast markers (*trnL-trnF*, *trnS-trnG* and *psbA-trnH*). Meseguer et al. (2013) analyzed different concatenated plastid data sets varying in the amount of missing data to evaluate its effect on phylogenetic reconstruction. Of these, we selected the matrix called "Two-markers" that only includes those specimens represented in at least two of the chloroplast markers ($N = 114$). The reduction in missing data allowed recovering a tree with higher resolution and branch support values than the complete data set including all specimens ($N = 192$), while at the same time recovering most of the morphological (92% of traditionally described sections) and all geographical variation within the genus (Robson 2012). The missing species mainly belong to the large *Brathys* group from America, *Ascyreia* from Asia, and the *Hirtella* group from the Levant region (Meseguer et al. 2013; Nürk et al. 2013a). Most species within these clades are distributed in the same biogeographic region, and all three clades are represented in our phylogeny. Moreover, Meseguer et al. (2013) used the "two-marker" data set in their biogeographic analysis based only on extant taxa, and using the same data set in this study facilitates comparison with their results. A fourth data set based on the nuclear marker ITS ($N = 252$) recovered a nearly identical tree than the plastid one (Meseguer et al. 2013), but was not used here because higher variation in substitution rates in nrDNA compared with chloroplast genes (Kay et al. 2006), and the possibility of incomplete concerted evolution in ITS (Álvarez and Wendel 2003) make this marker less reliable for phylogenetic dating. Four outgroup taxa representing the Cratoxyleae and Vismieae tribes in family Hypericaceae were also included in the analysis: *Harungana* Lamarck, *Psorospermum* Spach, and *Vismia* Vand. of the tropical tribe Vismieae sister to tribe Hypericeae and *Eliea* Cambess., representing the tropical tribe Cratoxyleae.

Phylogenetic relationships and absolute lineage divergence times within *Hypericum* were estimated in BEAST v.1.8.1 (Drummond et al. 2012). The "Two-marker" chloroplast data set was analyzed partitioned by-gene—that is, applying individual GTR+G substitution models to each gene—based on the results of Meseguer et al. (2013), who carried out sensitivity analyses to evaluate the effect of different partitioning strategies on their data. Choice of clock and tree model priors in the Meseguer et al. (2013) BEAST analysis was based on Bayes factor comparisons of the harmonic mean estimator of the posterior likelihood of alternative runs with different combinations of settings (e.g., strict clock vs. uncorrelated lognormal (UCLD), Yule vs. birthdeath). We repeated the analyses using the Path Sampling (PS) and Stepping Stone sampling methods, which have been shown to outperform the harmonic mean estimator in terms of reliability and consistency of results (Baele et al. 2012, 2013). We ran the analysis for 40 million generations, to which we added a chain length of 4 million generations as the power posterior runs. The highest likelihood corresponded to a birth-death tree prior with UCLD molecular clock, but this was not significantly higher than the Yule UCLD model (Table 1). Given that mixing, EES, and convergence were better in the latter model we used this model in our analysis with two replicate MCMC searches. As in Meseguer et al. (2013), two calibration points were used to derive absolute ages: the Late Eocene fossil *H. antiquum* to constrain the crown node of *Hypericum* (=Hypericeae) using a lognormal prior (offset = 33.9 myr, standard deviation "SD" = 0.7), and a secondary calibration point for the root of the tree (crown-node family Hypericaceae) from the calibrated clusioid clade phylogeny of Ruhfel (2011) applying a normal prior (mean = 65.2 myr, SD = 11) (see online Appendix 2 and Supplementary Fig. S1 in online Appendix 3 for more details).

TABLE 1. BEAST model comparison

	Strict-Yule	Strict-BD	Uncorrelated-Yule	Uncorrelated-BD
Path sampling	−3334.8355	−3334.3177	−2780.1459	−2780.1296
Stepping-stone	−3334.8206	−3334.3080	−2780.1439	−2780.1218

Notes: Marginal likelihood estimates for the concatenate "two-marker" data set of Meseguer et al. (2013) under different clock models (Strict/UCLD) and speciation processes (Yule/Birth-Death) based on PS and stepping-stone methods in BEAST v. 1.8.1.

Biogeographic Analysis

Biogeographic analyses were conducted with the DEC parametric likelihood method implemented in Lagrange (Ree et al. 2005; Ree and Smith 2008) using the fast C++ version (Smith 2009; https://github.com/rhr/lagrange-cpp). Species distributions were obtained from (Robson 1981-onwards). The world was divided into seven operational areas based on patterns of endemicity in *Hypericum* and the paleogeographic history of the continents Western Palearctic (WP), Eastern Palearctic (EP), Irano–Turanian–Himalayan region (ITH), Nearctic (NE), Oceania (OC), Africa (AF), and Neotropics (NT); a more detailed description on the delimitation of these areas is given in online Appendix 2. Widespread ancestral areas were limited to combinations of four areas, which is the maximum range of extant taxa.

To analyze the influence of fossils and ENM reconstructions (past and present environmental tolerances) in biogeographic inference, we set up four different analyses (M1–M4) in increasing order of complexity: (i) M1 used only distributions of extant species; (ii) M2 used present occurrences but incorporated a paleogeographic model with four time slices (60–35 Ma, 35–10 Ma, 10–3.5 Ma, 3.5–0 Ma; see online Appendix 2), representing major tectonic events hypothesized to have affected the migration rate of temperate plants (Donoghue and Smith 2004; Buerki et al. 2011); (iii) for M3 we used present occurrences and the same paleogeographic model to constrain area connectivity through time, but we integrated also the information provided by the fossil spatial ranges. The latter was done by constraining the ancestral range of crown node *Hypericum* to include the EP region, where the Late Eocene fossil *H. antiquum* was found. In this approach, fossil constraints placed on nodes are encoded as ancestral presence in the area containing the geographic locality of the fossil; Lagrange then calculates the likelihood of the data conditional on that area being included in the ancestral range at the node in question. This was done using existing functions in the C++ version, with the command "fossil = n mrca area", where *n* indicates a fossil assigned to constrain a node; "mrca" denotes the node defined by the function "mrca = mrcaname species1 species2"; and "area" designates the region where the fossil was found. Finally, (iv) M4 was identical to M3 but it also incorporated the information regarding the modeling of ancestral climatic preferences (fossil-based ENM). The ancestral area of the crown node was constrained to include the EP and NE regions; the latter is not represented in the fossil record, but ENM projections predicted it to be part of the potential distribution of *Hypericum* in the Late Eocene. In addition, we modified dispersal rates in the paleogeographic model to reflect variations in climatic adequacy for *Hypericum* across regions over time, such as the availability of transient migration corridors across unsuitable areas or climatic barriers that are specific to *Hypericum*. Thus, unlike the paleogeographic model in M2 and M3, dispersal probabilities in M4 reflected both the physical and "ecological" connectivity between regions. The latter was interpreted as the existence of regions with suitable climatic conditions according to the climatic tolerance of the group estimated for a given time period. More details on these models are given in online Appendix 2. Analyses were run on the maximum clade credibility tree from the MCMC BEAST analysis. Additionally, we ran the integrative M4 model over 1000 trees sampled from the BEAST posterior distribution to account for uncertainty in topology and branch length estimates. Changes in ancestral area inference resulting from model and phylogenetic uncertainty are presented in Supplementary Tables S2 and S3 in online Appendix 1, respectively.

Geographic-Dependent Extinction

We used the Geographic State Speciation and Extinction model "GeoSSE" (Goldberg et al. 2011) implemented in the R package *diversitree* (FitzJohn 2010) to investigate the existence of historical differences in speciation and extinction rates across biogeographic regions in *Hypericum*. In trait-dependent diversification models like GeoSSE or BISSE (Maddison et al. 2007), the trait itself (transitions between character states) influences the birth–death process that generates speciation times in the phylogeny. GeoSSE extends the BISSE binary model to incorporate a third, polymorphic state for geographic characters, since taxa are often not endemic but present in more than one area/state (Goldberg et al. 2011). Biogeographic regions were defined the same as above, except that we excluded the NT and OC from the analysis: the first does not include widespread species, whereas occurrence of *Hypericum* in OC is only marginal. For the selected geographic regions we estimated ML parameters for a full GeoSSE model—in which speciation, extinction

TABLE 2. Factor scores for the ENFA analysis of the study variables based on extant data

Climatic variables	F1	F2
Annual precipitation	0.528	0.204
Annual variation in precipitation	0.353	−0.037
Aridity	0.155	−0.644
Continentality	−0.314	−0.245
Maximum monthly precipitation	0.446	0.115
Maximum monthly temperature	−0.127	0.052
Mean annual temperature	0.109	0.179
Minimum monthly precipitation	0.448	0.015
Minimum monthly temperature	0.217	−0.659

Notes: Climatic variables selected as predictors were those showing the highest correlation values (factor scores >0.30) with the retained ENFA factors. Aridity and Continentality indices were calculated following the formulas provided by Valencia-Barrera et al. (2002).

and dispersal rate parameters are allowed to differ between areas—as well as for a set of GeoSSE constrained models: same rates of within-region speciation (sA ~ sB, sAB ~ 0), of between-region speciation (sAB ~ 0), of dispersal between regions (dA ~ dB) or of within-region extinction (xA ~ xB). Model fit comparison was assessed using likelihood ratio tests and comparing the Akaike Information Criterion values of the different models. The eight parameters estimated in the full GeoSSE model under ML were used as a prior for a Bayesian MCMC search. The MCMC chain was run for 10,000 generations, and the first 1000 were discarded. The current version of GeoSSE accounts for random incomplete taxon sampling within areas but can only manage two areas, so we compared each biogeographic region against the pooled values in all other regions, for instance, diversification and dispersal rates were estimated for species distributed in the EP region and compared with the values estimated for species in the remaining regions.

RESULTS

Environmental Niche Modeling

The ENFA analysis gave us two factors that explain 91.3% of total variability and 82.6% of specialization. The first ENFA factor was positively correlated with annual precipitation, annual variation in precipitation, and maximum and minimum monthly precipitation variables but negatively correlated with continentality (Supplementary Fig. S2 in online Appendix 3). The second factor was negatively correlated with aridity and minimum monthly temperature (Table 2; Supplementary Fig. S2). *Hypericum* marginality and specialization values were 0.54 and 2.46, respectively, indicating that the optimum climatic conditions for *Hypericum* were relatively near the average conditions available in the Earth, whereas the range of suitable conditions for *Hypericum* is more than two times narrower than those available on the planet.

Figure 2 shows the favorability of the world at different time periods for present (extant) and ancestral (fossil) *Hypericum* lineages. The percentage of terrestrial area with highly suitable habitat for *Hypericum* (MD <5, Q1, blue colors in the figure) oscillates between 23% in the Early Eocene, 29% in the Late Eocene, and 22% in the Early Miocene based on the "greenhouse" fossil optimum, and 13% (Late Miocene) and 26% (Pliocene) when based on the "coldhouse" fossil optimum. This percentage increases to 53% in the preindustrial world considering the extant species optimum (Fig. 2). Our models showed that—except for the Early Eocene period—the whole potential distribution of *Hypericum* could have remained relatively stable over the Cenozoic, showing a persistent presence of suitable climatic conditions over North America and Eurasia. In contrast, the tropical equatorial regions of South America, Africa, and Asia were as climatically unsuitable for *Hypericum* ancestral lineages (Fig. 2, high MDs) as they are today for their extant descendants. Similarly, hot and cold deserts would have been barriers for both present and extinct *Hypericum* lineages. During the warm and tropical Early Eocene period (Fig. 2a), only the northernmost areas showed suitable climatic conditions for *Hypericum* greenhouse ancestors, whereas the cooling event at the end of the Eocene created favorable conditions for these lineages in the intermediate latitudes of North America and Eurasia, including Beringia, and also in Australia, southern South America and the south of Africa (Fig. 2b). As the climate became gradually cooler from the Miocene onwards, the geographical area with favorable conditions for coldhouse ancestors increased (Fig. 2c–f), especially in the Pliocene and Preindustrial words, whereas the Late Miocene world marked a general reduction in geographic distribution (Fig. 2d). The Preindustrial world shows the highest percentage of area with favorable climatic conditions for *Hypericum*; the latter, however, could be partially an artifact produced by a much larger number of distribution occurrences and the coarse resolution of the paleoclimate models. Similar results were obtained after removing the intermediate Miocene fossils (Supplementary Fig. S3 in online Appendix 3).

When we examined the changes in the geographic area with favorable conditions for *Hypericum* through time and across biogeographic regions, we found that Asia experienced a dramatic decrease in favorable and intermediate conditions (Q1 and Q2 MD values, respectively) during the Late Miocene (Fig. 3). During the same period, the area with favorable conditions also decreased in the NE but intermediate conditions increased. Climatically suitable areas in all other regions remained relatively constant through time (Fig. 3).

Biogeographic Analyses

The four alternative biogeographic models reconstructed the ancestor of Hypericaceae (node 143) as African (Fig. 4, Supplementary Figs. S4–S7 in

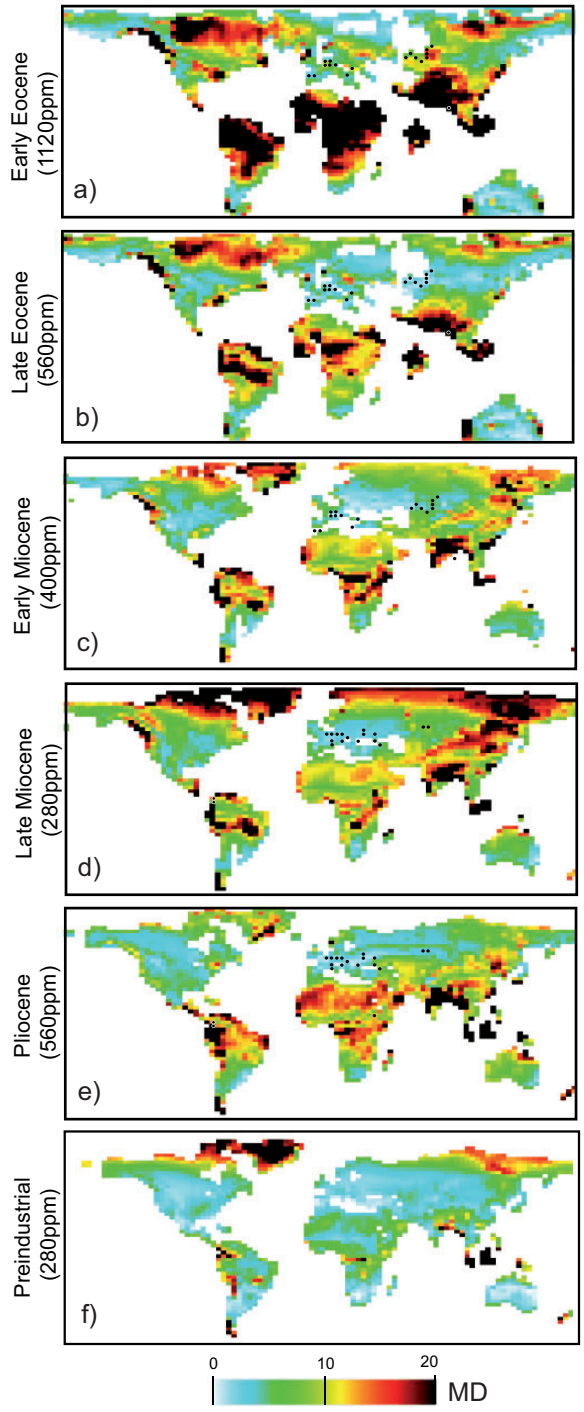

FIGURE 2. Potential distribution of *Hypericum* through time as inferred from fossil-based ENMs. A MD of 0 corresponds with the climatic optimum of *Hypericum*. Blue-green colors represent highly suitable habitat for *Hypericum* (MD <10). Red to black colors indicate climatically unsuitable regions for *Hypericum* (MD >10). These maps were created by projecting the climatic tolerances of extant and ancestral (fossil) *Hypericum* lineages onto six paleoclimate scenarios: Eocene-to-Early Miocene projections (a–c) were based on "greenhouse" fossil lineages, Late Miocene-to-Pliocene (d–e) on "coldhouse" fossil lineages, whereas the Preindustrial projection (f) was based on present occurrences. Dots represent the location of "greenhouse" and "coldhouse" fossil lineages in their respective maps (see text for more information).

online Appendix 3), but the timing of the first migration event to the Holarctic varies depending on which evidence is included (Supplementary Table S2, online Appendix 1). Models based on spatial distributions, either extant (M1 and M2) or fossil-extant (M3), inferred migration to the Holarctic along the branch leading to crown-group *Hypericum*, about 35 Ma (node 141, Supplementary Figs. S4–S6 in online Appendix 3). In contrast, the integrative M4 model that incorporates ecological connectivity among regions as derived from ENM predictions, reconstructed the stem-lineage of *Hypericum* (node 142) as already present in the Holarctic since the Early Eocene (ca. 50 Ma), whereas migration from AF is inferred earlier, along the branch leading to the ancestor of Hypericeae-Vismieae (Fig. 4). Another difference between models concerns the colonization of the EP region. Models based only on extant distributions (M1 and M2) reconstructed the ancestor of *Hypericum* as present in the WP, NE, and AF (node 141), whereas those models including the geographic range of the fossil *H. antiquum* (M3–M4) inferred crown-group *Hypericum* to be widespread in the entire Palearctic and NE regions (Fig. 4), with prior extinction in AF in model M3 (Supplementary Fig. S6). Fossil-based M3 model reconstructed the New World group as widespread in the EP region, whereas M4 inferred an extinction event in this area along the branch leading to the New World clade (node 36, Fig. 4). All models that incorporate a paleostratigraphic scenario inferred a recolonization of the EP in the Early Miocene (ca. 16 Ma) along the branch leading to the *Ascyreia* clade (node 71), whereas this is inferred later in the M1 model based on the extant distribution (node 70, ca. 12 Ma, Fig. 4). The latter model also indicates the persistence of several lineages in AF from the Paleocene to the present, whereas the paleogeographic-informed models (M2–M4) suggest later colonization during the Late Oligocene (Fig. 4 and Supplementary Figs. S4–S7).

Geographic-Dependent Extinction

The full model fitted the data better than the constrained models for all biogeographic regions, suggesting that diversification (speciation, extinction, and dispersal) has been range dependent in *Hypericum*. Nevertheless, differences between models were significant for only a few comparisons (Table 3), probably due to the small sample size of our phylogeny (see Davis et al. 2013). Although parameter values estimated for the different geographic regions are not directly comparable between areas (each area was evaluated independently against the rest of the world), our MCMC Bayesian estimates suggest that *Hypericum* lineages inhabiting the EP region have higher extinction and speciation rates (species turnover) than the lineages inhabiting the remaining regions (Fig. 5), although the comparison was not significant. Other regions, like ITH or WP, show the opposite pattern (lower speciation and extinction). Only AF shows posterior extinction rates

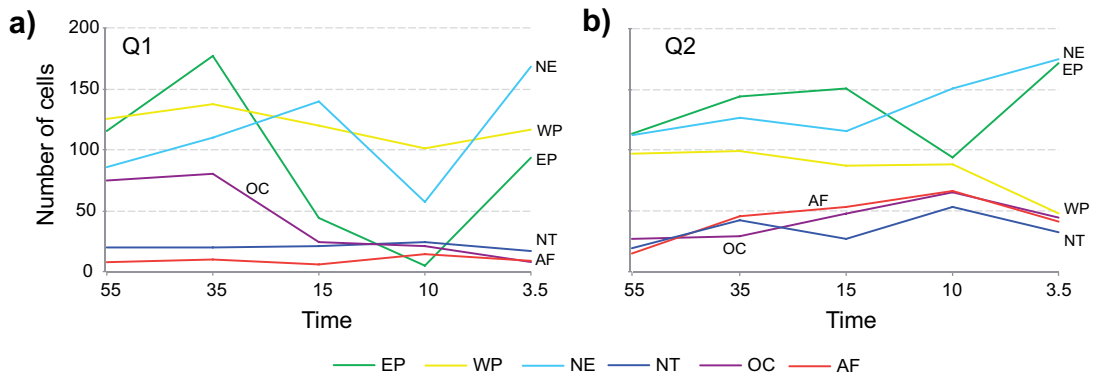

FIGURE 3. Evolution of area (number of cells with a resolution of 2.50°× 3.75°) with suitable climatic conditions for *Hypericum* through time and across biogeographic regions. a) Progression of the most favorable conditions through time (Q1). b) Progression of the intermediate conditions (Q2). Line colors correspond with the discrete areas defined in the inset map of Figure 4. Color version of this figure is available at *Systematic Biology* online.

slightly higher than in the rest of the world, but mean values are very close and there is considerable overlap (Fig. 5). Interestingly, the between-regions speciation parameter (sAB) is high in all regions, especially in ITH, suggesting a high frequency of vicariance and peripatric isolation events in the history of the group (Table 3).

DISCUSSION

Biogeography has traditionally been regarded as an integrative discipline, at the meeting point of geology, paleontology, systematics, and ecology. Early biogeographers such as Joseph D. Hooker (1867) or Alfred Wallace (1876) blended in their works information sources as diverse as the fossil record, geology, or paleoclimatology (Lomolino et al. 2010). This integrative view was somewhat lost with the rise and dominance of the cladistic biogeography school and its search for patterns of area relationships or area cladograms (Wiens and Donoghue 2004; Sanmartín 2012). The recent development of parametric methods that can integrate time into biogeographic reconstructions has allowed geological and paleogeographic information to regain its role in biogeographic inference (Buerki et al. 2011). Two other sources of evidence, the fossil record and ecology, have proven more difficult to integrate, but as we will see below, they provide crucial information in historical biogeographic studies.

Fossils Place Ancestors in Space and Time

The importance of fossils in biogeography was emphasized by paleontologists like Lieberman (2002, 2003), who compared it with the effect of incomplete taxon sampling in phylogenetic inference. Failing to include all representatives within a clade can lead to biased estimates of divergence times (Linder et al. 2005) or of evolutionary history (Litsios and Salamin 2012). Extinction causes a similar effect in biogeography. When the geographic ranges of extinct taxa are not included in the analysis, spurious reconstructions and artificially incongruent distribution patterns are likely to be obtained (Lieberman 2005). The approach we present here incorporates the geographic information provided by fossils directly into Lagrange biogeographic analyses by constraining the inference of ancestral areas in those nodes calibrated with the fossil record to include the spatial range of fossils. This avoids making assumptions about the length duration (longevity) of the fossil (Nauheimer et al. 2012), or the need to code fossil morphological characters for every extant taxa or introducing missing data for all molecular characters in the fossil (Mao et al. 2012). To our knowledge, this is the first empirical study using this fossil functionality in Lagrange.

Integrating the spatial range of the oldest fossil of *Hypericum* (*H. antiquum* from West Siberia) in the biogeographic analysis resulted in the EP being inferred as part of the ancestral distribution of several basal nodes in the phylogeny—that is, the ancestor of the tribes Hypericeae and Vismieae (Node 142), the crown node of *Hypericum*, the ancestor of all extant sections excepting *Elodes-Adenotrias* (Node 140), and the ancestor of the New World group (Node 141 in M3, Fig. 4)—in agreement with the fossil record (Fig. 1b; Supplementary Table S1). This contrasts with reconstructions based only on present-day distributions (Meseguer et al. 2013, M1 and M2 in Fig. 4), in which the EP is colonized in more recent times (Miocene). However, even the fossil-based reconstructions M3 and M4 failed to show a continuous presence in the EP, as otherwise supported by the fossil record: they indicate an ancestral presence in the EP during the Eocene–Oligocene, disappearance from the area and posterior recolonization of this region in the Early Miocene (Fig. 4).

We do not think that the incongruence found between the fossil record and our biogeographic reconstructions is an artifact of the biogeographic method, because the Bayesian diffusion approach (Lemey et al. 2009) used by Meseguer et al. (2013) and our own DEC analyses (M1 and M2) infer similar results. Incomplete taxon

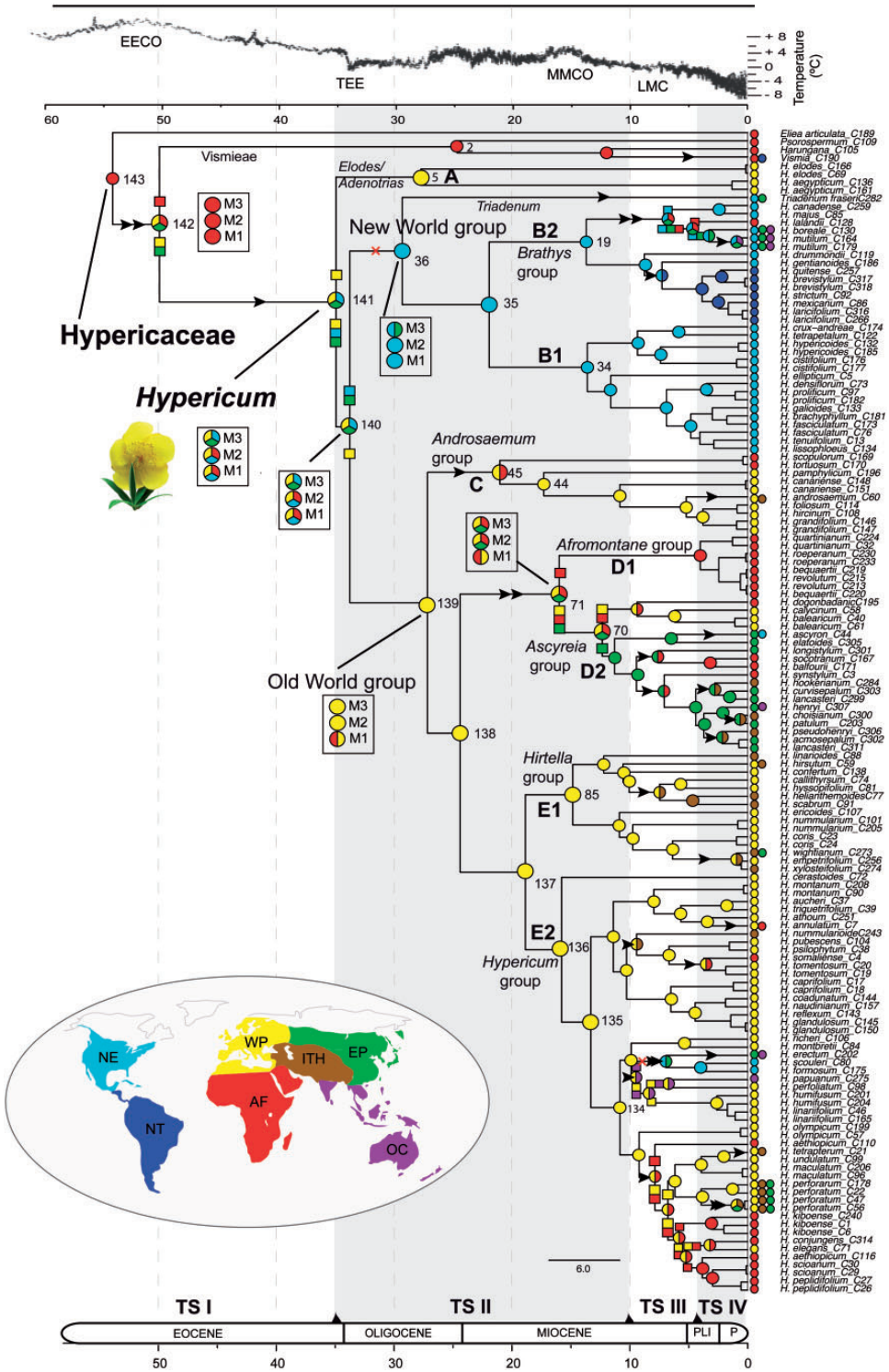

FIGURE 4. Reconstruction of the spatio-temporal evolution of *Hypericum* showing the effects of the sequential incorporation of additional sources of information (paleogeographic, fossil and ecological preferences) into biogeographic inference. M1 results are based on a biogeographic analysis using only the distribution of extant taxa. M2 adds a paleogeographic model to reflect continental connectivity through time. Time slices (TSs) indicated by grey vertical bars. M3 incorporates fossil ranges. M4 (main figure) combines all these sources but further integrates estimations of ancestral potential distributions and predicted ecological corridors from the fossil-based ENM models (Fig. 2). M1–M3 results are only shown for those nodes whose reconstruction differs between models. Ancestral ranges (colored pie charts), range division scenarios (square splits), dispersal events (arrows), and extinction events (red crosses) were inferred with Lagrange (Ree and Smith 2008) over the dated phylogeny of Meseguer et al. (2013) and 1000 trees from the posterior distribution (see text for more details). Colored circles before the species names give present ranges; color codes for nodes and terminal taxa correspond with the discrete areas in the inset map. Global mean temperature curve at the top of the figure modified from Zachos et al. (2008). Node numbers correspond with those of Supplementary Tables S2 and S3. Clade names "A–E" represent major lineages recovered by Meseguer et al. (2013). Abbreviations: EECO, Early Eocene Climatic Optima; TEE, Terminal Eocene Event; MMCO, Mid-Miocene Climatic Optimum; LMC, Late Miocene cooling; PLI, Pliocene; P, Pleistocene. Areas: AF (Sub-Saharian Africa), WP (western Palearctic), EP (eastern Palearctic), IT (Irano-Turanian-Himalayan), OC (Oceania), NE (Nearctic), and NT (Neotropic).

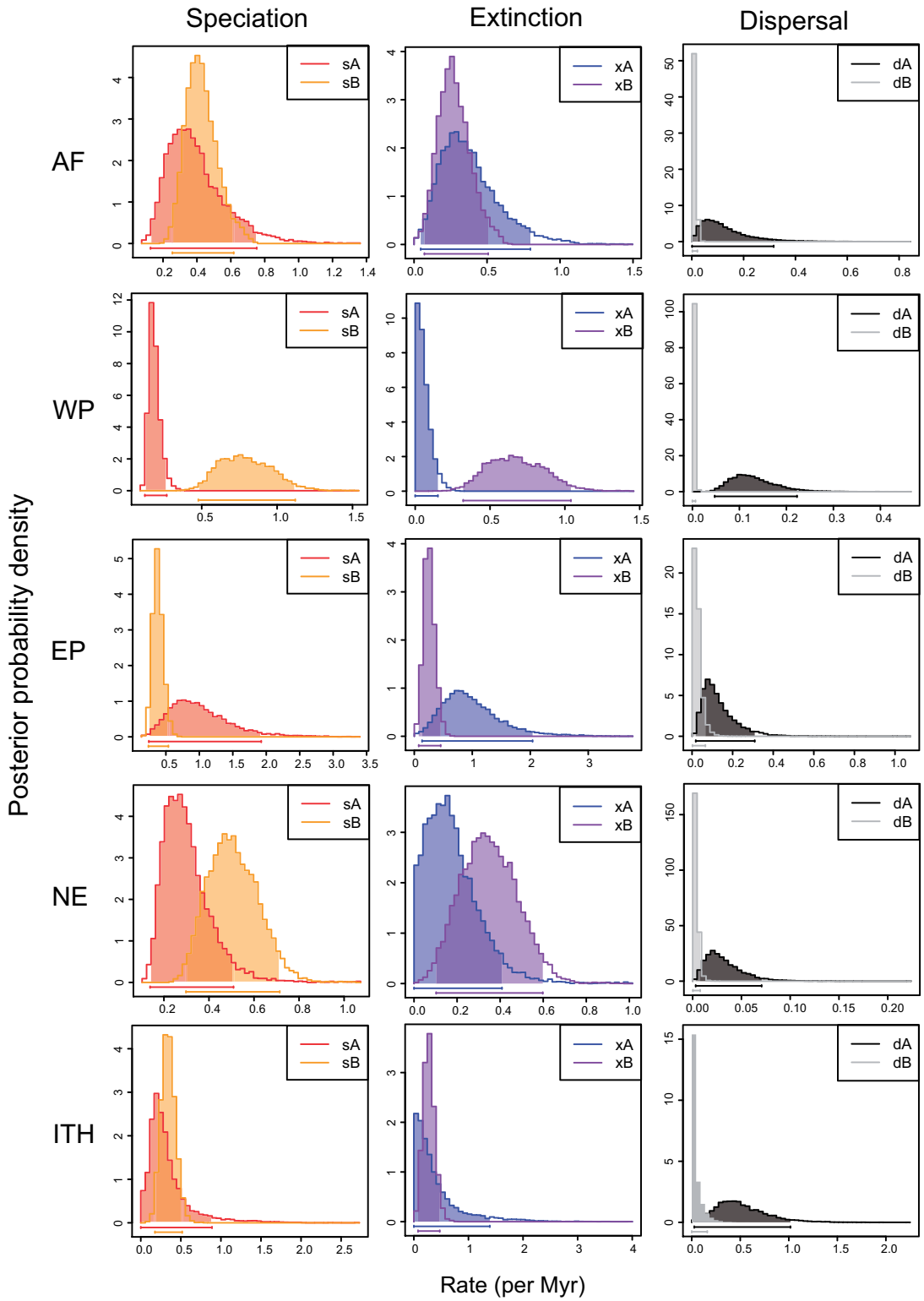

FIGURE 5. GeoSSE analysis. Posterior probability distributions estimated by Bayesian MCMC analysis for the GeoSSE "full model." Speciation, extinction, and dispersal values are shown for each focal region (*s*A, *x*A, and *d*A, respectively) against the pooled values of the other biogeographic regions (*s*B, *x*B, and *d*B); see text for more details. Abbreviations: *d*A, dispersal from A to B; *d*B, dispersal from B to A; AF, Sub-Saharian Africa; WP, western Palearctic; EP, eastern Palearctic; IT, Irano-Turanian-Himalayan; OC, Oceania; NE, Nearctic; NT, Neotropic. Color version of this figure is available at *Systematic Biology* online.

TABLE 3. GeoSSE results for the concatenate "two-marker data set" of Meseguer et al. (2013)

		*s*A	*s*B	*s*AB	*x*A	*x*B	*d*A	*d*B
EP	ML	0.762	0.344	1.532	0.669	0.201	0.090	0.016
	Bayes	1.007 (0.57)	0.35 (0.07)	2.53 (1.96)	0.98 (0.62)	0.22 (0.09)	0.14 (0.09)	0.03 (0.02)
WP	ML	0.150	0.731	1.036	0.000	0.607	0.119	0.002
	Bayes	0.187 (0.04)	0.79 (0.17)	1.31 (0.96)	0.058 (0.05)	0.67 (0.19)	0.129 (0.05)	0.003 (0.0)
IT	ML	0.150	0.279	12.101	0.000	0.287	0.765	0.000
	Bayes	0.335 (0.28)	0.344 (0.09)	6.14 (2.95)	0.406 (0.45)	0.276 (0.1)	0.506 (0.26)	0.043 (0.06)
AF	ML	0.299	0.426	5.219	0.265	0.268	0.095	0.008
	Bayes	0.398 (0.17)	0.427 (0.09)	3.38 (2.29)	0.383 (0.2)	0.27 (0.11)	0.127 (0.09)	0.01 (0.005)
NE	ML	0.238	0.475	0.240	0.100	0.312	0.020	0.002
	Bayes	0.302 (0.11)	0.508 (0.11)	1.415 (1.49)	0.179 (0.12)	0.35 (0.131)	0.032 (0.02)	0.003 (0.00)

Notes: Maximum likelihood and Bayesian parameters (mean and SD) under the full GeoSSE model for each biogeographic comparison. Biogeographic regions are shown in bold in those cases in which the full GeoSSE model was significantly better than the constrained models; in all other cases the full model fitted the data better but differences between models were not significant. Abbreviations: *s*A, speciation rate for area A, *x*A, extinction rate for area A; *d*A, dispersal rate, *s*AB, speciation rate for widespread area AB, where area A represents the focal area and B the other areas pooled together. Code for areas follows Figure 4.

sampling in our phylogeny cannot explain this, either, since EP is actually poorly represented across extant *Hypericum* clades. Nowadays, the northern part of this regions, where most fossils are found, harbors only a few widespread species, whereas the majority of EP extant lineages are restricted to southern areas like southern China or the Himalayas, for example, the *Ascyreia*-group (Robson 1981). Moreover, our phylogenetic sampling included a good representation of these EP lineages, that is, species from sections *Ascyreia*, *Roscyna*, *Takasagoya*, *Monanthema*, and *Hypericum.*

A more likely explanation supported by our study is that high extinction rates in the EP region—associated with the global climate cooling that started in the Late Cenozoic—are responsible for the disagreement between the fossil record of *Hypericum* and our biogeographic reconstructions. GeoSSE results suggested that speciation and extinction rates in EP have been considerably higher than in the rest of the world (Fig. 5), and our fossil-based ENM projections showed a dramatic decrease in climatically suitable areas in the EP during the Late Cenozoic (Fig. 3). A higher extinction rate in this region might seem surprising, since Asia has traditionally been considered a refuge for temperate "mixed-mesophytic" lineages during the climatic shifts of the Late Cenozoic that extirpated this forest from Europe and Western North America (Tiffney 1985a, 1985b; Sanmartín et al. 2001; Donoghue and Smith 2004). One explanation is that the high extinction rates inferred here refer only to the northernmost part of the EP region. Our fossil-based bioclimatic models indicate that the southeastern regions of Asia, where the *Ascyreia* lineage (Clade D) is now distributed, were climatically favorable for *Hypericum* throughout its Cenozoic history (Fig. 2). It is thus possible that *Ascyreia* is a relict group of this former widespread EP distribution and not the result of a Miocene colonization event from Europe. The finding of Miocene fossil remains of *Hypericum* in what is considered a relict assemblage of the temperate mixed-mesophytic forest in Yunnan, China (Meseguer and Sanmartín 2012) supports an earlier presence in this area. This hypothesis could be tested by adding to the analysis more fossil data from the EP region in addition to the Late Eocene *H. antiquum.* Unfortunately, lack of taxonomic characters in these fossils (see Methods) meant that we could not confidently assign any of them to extant clades, and therefore could not take full advantage of the spatial information provided by the fossil record of *Hypericum*. Nevertheless, some of these fossils were useful to corroborate *a posteriori* the inferences made by the biogeographic analyses. For example, for some regions like South America or Africa, the age of the oldest recorded (pollen) fossil—Pliocene according to Meseguer and Sanmartín (2012)—is in agreement with the time when these regions were first colonized as inferred in our biogeographic analyses (Fig. 4). On the other hand, absence of fossil remains does not necessarily imply a late colonization event, since the fossil record might be biased toward certain regions simply because of higher fossilization potential or more paleontological work being done in those regions. For example, the fossil record of the Nearctic does not begin until the Pleistocene (Meseguer and Sanmartín 2012), but fossil-based ENM models predict favorable conditions in this region throughout the entire Cenozoic, and our biogeographic analyses recovered the NE as part of the ancestral distribution of the genus (Figs. 2 and 4). This emphasizes the importance of an integrative approach that jointly considers different sources of information in the inference of biogeographic history.

Fossils Contain Information on Ancestral Climatic Preferences

By integrating ecological information from past and extant lineages in our fossil-based bioclimatic models, we were able to identify climatic corridors and barriers to dispersal that were specific to *Hypericum* and shaped its evolutionary trajectory over space and time. For any organism, the presence of a physical landbridge is not

the only requisite for its dispersal; the environmental conditions along the bridge must be also within the climatic tolerances of the organism (Donoghue 2008). Similarly, range division does not necessarily result only from the rising of a geological barrier, but can also be the outcome of any climatic change that causes the loss of suitable habitat (Wiens and Donoghue 2004). Donoghue (2008) argued that the interplay between changing geographic intercontinental connections and climatic fluctuations through the Cenozoic has determined the availability of migration routes to plants, ultimately resulting in many of the global-scale distribution patterns we observe today.

During the Cenozoic, land dispersal of temperate plants between the Palearctic and NE regions involved two main migratory routes: the North Atlantic Land Bridge (NALB) and the Beringian Land Bridge (BLB) (Tiffney 1985a). The NALB is thought to have been the main dispersal corridor between Eurasia and North America during the Early Cenozoic, peaking after the Early Eocene Warming Event, whereas the Beringian Bridge became the most important route after the Terminal Eocene cooling event (Sanmartín et al. 2001; Tiffney 1985a, 1985b). Our fossil-based ENM models show that the NALB has never been climatically favorable for *Hypericum*, and that dispersal events between Nearctic and Palearctic during the Cenozoic probably involved the BLB (Fig. 2). The cooling event in the Late Miocene interrupted this Beringian connection (Fig. 2d), but it was regained during the warm Mid-Pliocene interval (Fig. 2e), in which cool temperate deciduous forests expanded northwards, at the expense of the taiga and tundra vegetation (Salzmann et al. 2008). The biogeographic reconstruction shows several dispersal events followed by allopatric speciation (vicariance) between Nearctic and Palearctic regions dated around this period (e.g., *Hypericum ascyron*, Fig. 4). Interestingly, our bioclimatic models indicate that the southern temperate regions of Australia, Africa and South America presented favorable conditions for *Hypericum* throughout its evolutionary history (Fig. 2a–f). This stands in contrast with the current low diversity of these regions, which, except for Africa harbor mainly widespread species present in other continents. During the Late Cenozoic, these three southern continents, which once formed part of the supercontinent of Gondwana, moved closer to the Holarctic landmasses (Australia, Africa) or became geographically connected, that is, South America through the Isthmus of Panama. The presence of the tropical equatorial belt in South America and Southeast Asia, however, seems to have acted as a climatic barrier, preventing *Hypericum* lineages from reaching the southern temperate regions of these continents (Fig. 2). In contrast, the aridification process that affected Africa from the Miocene onwards, and led to the replacement of tropical forests by woodlands and savannah in the north, east, and south of the continent (Senut et al. 2009), might have generated an ecological corridor that allowed *Hypericum* lineages to migrate to the south (Fig. 2c–d). Increasing aridification during the Pliocene broke this connection and led to the formation of large deserts across North Africa and Arabia (Fig. 2e). However, during this period, a new corridor was probably formed with the rising of mountain ranges in East AF (the Eastern Arc Mountains) and South America (the northern Andes), providing *Hypericum* lineages with adequate temperate habitats along the peaks and slopes of the mountains to move southwards, for example, the Andean clade in section *Brathys* or the South African radiation in section *Hypericum* (Meseguer et al. 2013; Nürk et al. 2013b). The coarse resolution of our fossil-based climate models—a necessary trade-off when these models are used at a worldwide scale and over longer periods of Earth history—does not allow us to test this hypothesis, for example, mountain ranges were not discriminated against the surrounding habitat (Fig. 2e). Nevertheless, our biogeographic reconstruction (Fig. 4) inferred several events of dispersal followed by diversification that are concurrent with the rising of the Neogene mountain chains; for example, entrance into South America in the *Brathys* clade (Fig. 4) is dated around the Pliocene, contemporary with the elevation of the northern Andes (Hoorn et al. 2010).

Spatio-temporal Evolution of Hypericum: Evidences from an Integrative Approach

The Cenozoic period—the last 65 million years of Earth history—have been characterized by major changes in continental configuration and rapid and large shifts in global climate (Zachos et al. 2008; Scotese 2010). Reconstructing the evolution of a lineage in this unstable world requires the integration of different sources of evidence: biogeographic (where did they come from?), temporal (when did they originate?), and ecological (which were the climatic conditions under which ancestral lineages evolved?).

Fifty-five million years ago, the Earth experienced one of the warmest intervals in history, with global temperatures up to 10°warmer than present and tropical climates characterizing northern latitudes (Zachos et al. 2008). The boreotropical flora, a mixture of hardwood deciduous and evergreen tropical taxa with no analog today, extended across North America and Eurasia (Fig. 6a, Tiffney 1985, Wolfe 1975). The ancestors of family Hypericaceae probably migrated from Africa to the Palearctic region during this warm Paleogene period and might have formed part of this boreotropical flora about 50 million years ago (Node 142, Fig. 4). Our bioclimate model for the Early Eocene, however, does not support this scenario, showing that the tropical regions of the Southern Hemisphere and a large area in the Holarctic where, the boreotropical forest was distributed (Fig. 6a), as climatically unfavorable (Fig. 2a). Nevertheless, the fossil record of *Hypericum* only extends back to 35 Ma, and the Early Eocene bioclimatic model is only based on Late Eocene to Mid-Miocene occurrences. Thus, it is possible that this ENM reconstruction does not correctly represents the potential

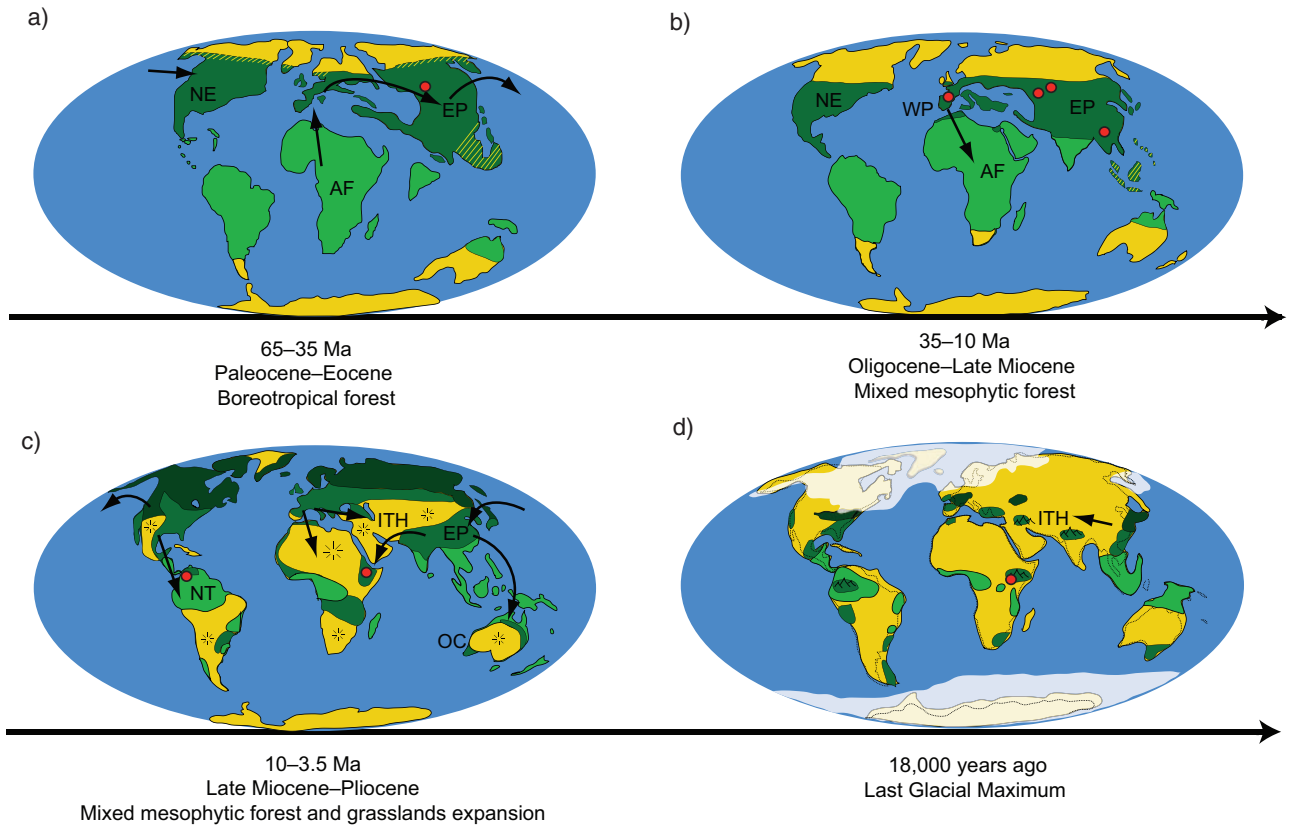

FIGURE 6. Scheme representing changes in vegetation composition in response to major shifts in Cenozoic climate based on paleobotanical evidence (see online Appendix 2 for more details on how the vegetation maps were constructed), together with the biogeographic history of genus *Hypericum* as inferred from the integrative approach adopted here (Fig. 4). The close-canopy tropical forest in the Southern Hemisphere is represented by light green color over a yellow background. The northern vegetation belt in dark green color represents alternatively the boreotropical forest (Fig. 6a), and its successors: the mixed-mesophytic forest (Fig. 6b,c) and the temperate forest (Fig. 6d). The boreal forest belt in the northern regions of Eurasia and North America (Fig. 6c,d) is represented by a darker shade of green; starbursts represent the expansion of grassland biomes. Red dots represent selected fossil locations. Area name abbreviations follow Figure 4.

distribution of *Hypericum* stem-lineages, if they were adapted to more tropical conditions than their temperate descendants.

The first diversification event within *Hypericum* (crown-node), and the colonization of the Nearctic—likely through Beringia—coincided with the global climate cooling at the Eocene–Oligocene boundary (ca. 35 Ma, Fig. 4). The TEE promoted the selection of cold-temperate elements in the boreotropical vegetation and the expansion of a deciduous mixed-mesophytic forest, whereas evergreen boreotropical taxa became extinct or migrated southwards (Wolfe 1975, 1985; Fig. 6b). Our bioclimatic model for the Late Eocene period (Fig. 2b) shows a geographic area with suitable climatic conditions for *Hypericum* that is to a large extent coincident with the distribution of the mixed-mesophytic forest (Fig. 6b). The period that followed the TEE was characterized by rapid climatic oscillations between periods of warm and humid climate and dry and colder episodes (Zachos et al. 2008). Back-dispersal into the Southern Hemisphere regions could have happened during the Miocene and involved the ancestors of the *Androsaemum* (clade C) and *Ascyreia*-Afromontane groups (clade D) colonizing sub-Saharan Africa (Figs. 4 and 6b), probably facilitated by the aridification of the continent that started in this period (Fig. 2c,d). The LMC event (ca. 10 Ma, Zachos et al. 2008) led to the displacement of the mixed-mesophytic vegetation by a boreal coniferous forest through the northern regions of North America and Eurasia, and to the expansion of grasslands in the inner continental areas of these regions (Fig. 6c). Our fossil-based ENM models for coldhouse lineages indicate a decrease in the proportion of climatically suitable habitat for *Hypericum* after the LCM (Figs. 2d and 3), especially across Beringia, the Eastern Palearctic, and the northern regions of North America, following the retreat of the mixed-mesophytic forest (Fig. 6c). The Warm Mid-Pliocene interval (3.5 Ma) coincided with an increase in the geographic area with suitable climatic conditions for *Hypericum*, especially across Beringia. During this period, some *Hypericum* lineages probably used the climatic corridors provided by the newly uplifted Andean and Eastern African mountains to disperse again to the south (Fig. 4). During the Pleistocene (Fig. 6d), ice sheets covered large regions of Eurasia and North America and a tundra

belt extended across Beringia while temperate plants became restricted to climatic refugia in the south. This reduction in geographic distribution cannot be seen in our bioclimatic model for the Preindustrial world (Fig. 2e), but could be responsible for some of the geographic disjunctions we observe today in *Hypericum*, such as sister species distributed on each side of Beringia (e.g., *Triadenum walteri and Triadenum japonicum*) or the same species occurring on both sides of the central-African tropical belt, for example, *Hypericum revolutum* (Meseguer et al. 2013).

One of the most surprising results from our analysis is the fact that the geographic distribution of *Hypericum* as a genus has remained relatively stable through the dramatic climatic oscillations of the Cenozoic. Despite the range contractions and expansions described above, *Hypericum* crown ancestors inhabited geographic regions in the Holarctic similar to those their extant descendants now occupy, for example, they could not live in cold and hot deserts or in the lowland tropical equatorial regions. Whether this can be explained by rapid adaptation to the changing climatic conditions or by a remarkable degree of niche conservatism (Peterson 2011) is a question that should be further studied. Moreover, our ENM projections can only show the potential distribution of *Hypericum*, that is, the *a priori* climatically suitable areas that could be inhabited by species in the absence of significant dispersal limitations, local extinctions, or competitive exclusion. Only by including these bioclimatic models into a biogeographic analysis were we able to approximate the past "realized" distribution of the genus, that is, when and where each major lineage originated and the time of occupancy of each area.

Conclusions

Our study shows that a biogeographic approach that combines different sources of evidence, such as the fossil record, paleoclimatic data, and phylogenetic relationships, provides more realistic inferences of the past, helping to minimize the biases associated with each separate source of information. Our integrative approach blends traditionally independent disciplines like ecology, paleontology, and phylogenetics into a common research program. Although this has just started to be explored in demographic models for the recent past (Metcalf et al. 2014), this approach is probably more critical for a deep-time perspective. In many cases, the biodiversity we observe today is not representative of the past diversity, and using present-day distributions for inferring the past is even more dangerous when one is dealing with geological time scales of tens or hundreds of million years. Our study also highlights the confounding effect that different rates of extinction across regions can have in biogeography, which might result in extant marginal distributions like the Eastern Palearctic being incorrectly inferred as resulting from recent dispersal rather than as part of the lineage's ancestral distribution as otherwise supported by the fossil record.

Author's Contribution

I.S., A.S.M., and J.M.L. designed the study; A.S.M. and I.S. collected the data; A.S.M., I.S., J.M.L., and R.R. analyzed the data; D.J.B. provided the climatic data; and A.S.M. and I.S. wrote the paper with contributions from J.M.L.

Supplementary Material

Data available from the Dryad Digital Repository: http://dx.doi.org/10.5061/dryad.5845b.

Acknowledgments

This work is based on the PhD thesis of A.S.M. defended in 2013. The authors are indebted to J. Fuertes, G. Nieto, L. Pokorny, and E. Jousselin for useful suggestions to early drafts of the manuscript. They thank L. Taylor for technical support in relation to the global climate data sets, and C. Bradshaw, D. Lunt, and P. Valdes for their earlier modeling of Cenozoic climates. They also thank F. Anderson (Editor-in-Chief), A. Mast (Associated Editor), and two anonymous reviewers for their valuable comments, which greatly helped improve the manuscript.

Funding

This work was supported by grants from the Spanish Ministry of Science and Innovation, CBG2009-13322-C01 and CGL2012-43329-C01, to I.S. and CBG2010-24555 to J.M.L., and a PhD grant, AP-2007-01698, to A.S.M.

References

Aarts G., Fieberg J., Matthiopoulus J. 2011. Comparative interpretation of count, presence–absence and point methods for species distribution models. Methods Ecol. Evol. 3:177–187.

Álvarez I., Wendel J.F. 2003. Ribosomal ITS sequences and plant phylogenetic inference. Mol. Phylogenet. Evol. 29:417–434.

Arbuzova O. 2005. *Hypericum* L. In: Budantsev L., editor. Iskopaemye tsvetkovye rastenija Rossii i sopredel'nyh gosudarstv [Fossil flowering plants of Russia and adjacent countries]. Leningrad, Izdatelstvo Nauka Leningradskoe otdnie, 1974.

Baele G., Lemey P., Bedford T., Rambaut A., Suchard M.A., Alekseyenko A.V. 2012. Improving the accuracy of demographic and molecular clock model comparison while accommodating phylogenetic uncertainty. Mol. Biol. Evol. 9:2157–2167.

Baele G., Li W.L.S., Drummond A.J., Suchard M.A., Lemey P. 2013. Accurate model selection of relaxed molecular clocks in Bayesian phylogenetics. Mol. Biol. Evol. 30:239–243.

Barrón E., Rivas-Carballo R., Postigo-Mijarra J.M., Alcalde-Olivares C., Vieira M., Castro L., Pais J., Valle-Hernández M. 2010. The Cenozoic vegetation of the Iberian Peninsula: a synthesis. Rev. Palaeobot. Palynol. 162:382–402.

Beaumont L.J., Hughes L., Poulsen M. 2005. Predicting species distributions: use of climatic parameters in BIOCLIM and its impact

on predictions of species' current and future distributions. Ecol. Model. 186:251–270.
Beerling D., Berner R.A., Mackenzie F.T., Harfoot M.B., Pyle J.A. 2009. Methane and the CH4 related greenhouse effect over the past 400 million years. Am. J. Sci. 309:97–113.
Beerling D.J., Fox A., Stevenson D.S., Valdes P.J. 2011. Enhanced chemistry-climate feedbacks in past greenhouse worlds. Proc. Natl Acad. Sci. U. S. A. 108:9770–9775.
Beerling D.J., Royer D.L. 2011. Convergent Cenozoic CO_2 history. Nat. Geosci. 4:418–420.
Beerling D.J., Taylor L.L., Bradshaw C.D.C., Lunt D.J., Valdes P.J., Banwart S.A., Pagani M., Leake J.R. 2012. Ecosystem CO_2 starvation and terrestrial silicate weathering: mechanisms and global-scale quantification during the late Miocene. J. Ecol. 100:31–41.
Bonnefille R., Vincens A., Buchet G. 1987. Palynology, stratigraphy and palaeoenvironment of a Pliocene hominid site (2.9–3.3 M.Y.) at Hadar, Ethiopia. Palaeogeogr. Palaeoclimatol. Palaeoecol. 60:249–281.
Bradshaw C.D., Lunt D.J., Flecker R., Salzmann U., Pound M.J., Haywood A.M., Eronen J.T. 2012. The relative roles of CO_2 and palaeogeography in determining late Miocene climate: results from a terrestrial model–data comparison. Clim. Past 8:1257–1285.
Buerki S., Forest F., Alvarez N., Nylander J.A.A., Arrigo N., Sanmartín I. 2011. An evaluation of new parsimony-based versus parametric inference methods in biogeography: a case study using the globally distributed plant family Sapindaceae. J. Biogeogr. 38:531–550.
Calenge C., Basille M. 2008. A general framework for the statistical exploration of the ecological niche. Amsterdam: Elsevier.
Cavagnetto C., Anadón P. 1996. Preliminary palynological data on floristic and climatic changes during the Middle Eocene–Early Oligocene of the eastern Ebro Basin, northeast Spain. Rev. Palaeobot. Palynol. 92:281–305.
Clarke G. 1981. Pollen morphology. Studies in the genus *Hypericum* L. (Guttiferae) 2. Characters of the genus. Bull. Br. Mus. Nat. Hist. (Bot.) 8:115–118.
Corner E.J.H. 1976. The seeds of dicotyledons. Vols. 1, 2. Cambridge: Cambridge University Press.
Davis M.P., Midford P.E., Maddison W. 2013. Exploring power and parameter estimation of the BiSSE method for analyzing species diversification. BMC Evol. Biol. 13:38.
Donoghue M.J. 2008. A phylogenetic perspective on the distribution of plant diversity. Proc. Natl Acad. Sci. U. S. A. 105:11549–11555.
Donoghue M.J., Smith S.A. 2004. Patterns in the assembly of temperate forests around the Northern Hemisphere. Philos. Trans. R. Soc. Lond. B Biol. Sci. 359:1633–1644.
Drummond A.J., Suchard M.A., Xie D., Rambaut A. 2012. Bayesian phylogenetics with BEAUti and the BEAST 1.7. Mol. Biol. Evol. 29:1969–1973.
FitzJohn R.G. 2010. Quantitative traits and diversification. Syst. Biol. 59:619–633.
Goldberg E.E., Lancaster L.T., Ree R.H. 2011. Phylogenetic inference of reciprocal effects between geographic range evolution and diversification. Syst. Biol. 60:451–465.
Hastie T., Fithian W. 2013. Inference from presence-only data; the ongoing controversy. Ecography 36:864–867.
Hedberg O. 1954. A pollen-analytical reconnaissance in tropical East Africa. Oikos 5:137–166.
Hijmans R.J., Cameron S.E., Parra J.L., Jones P.G., Jarvis A. 2005. Very high resolution interpolated climate surfaces for global land areas. Int. J. Climatol. 25:1965–1978.
Hirzel A.H., Hausser J., Chessel D., Perrin N. 2002. Ecological-niche factor analysis: how to compute habitat-suitability maps without absence data? Ecology 83:2027–2036.
Ho S.Y.W., Phillips M.J. 2009. Accounting for calibration uncertainty in phylogenetic estimation of evolutionary divergence times. Syst. Biol. 58:367–380.
Hooker J.D. 1867. Lecture on insular floras. London, Delivered before the British Association for the Advancement of Science at Nottingham.
Hoorn C., Wesselingh F.P., Ter Steege H., Bermudez M.A., Mora A., Sevink J., Sanmartín I., Sanchez-Meseguer A., Anderson C.L., Figueiredo J.P., Jaramillo C., Riff D., Negri F.R., Hooghiemstra H., Lundberg J., Stadler T., Särkinen T., Antonelli A. 2010. Amazonia through time: Andean uplift, climate change, landscape evolution, and biodiversity. Science 330:927–931.
Janeček Š., Hrázský Z., Bartoš M., Brom J., Reif J., Hořák D., Bystřická D., Riegert J., Sedláček O., Pešata M. 2007. Importance of big pollinators for the reproduction of two *Hypericum* species in Cameroon, West Africa. Afr. J. Ecol. 45:607–613.
Jiménez-Valverde A., Peterson A.T., Soberón J., Overton J.M., Aragón P., Lobo J.M. 2011. Use of niche models in invasive species risk assessments. Biol. Invasions 13:2785–2797.
Kay K.M., Whittall J.B., Hodges S.A. 2006. A survey of nuclear ribosomal internal transcribed spacer substitution rates across angiosperms: an approximate molecular clock with life history effects. BMC Evol. Biol. 6:36.
Lemey P., Rambaut A., Drummond A., Suchard M. 2009. Bayesian phylogeography finds its roots. PLoS Comput. Biol. 5:e1000520–e1000520.
Lieberman B.S. 2002. Phylogenetic biogeography with and without the fossil record: gauging the effects of extinction and paleontological incompleteness. Palaeogeogr. Palaeoclimatol. Palaeoecol. 178:39–52.
Lieberman B.S. 2003. Paleobiogeography: the relevance of fossils to biogeography. Annu. Rev. Ecol. Evol. Syst. 34:51–69.
Lieberman B.S. 2005. Geobiology and paleobiogeography: tracking the coevolution of the Earth and its biota. Palaeogeogr. Palaeoclimatol. Palaeoecol. 219:23–33.
Linder H.P., Hardy C.R., Rutschmann F. 2005. Taxon sampling effects in molecular clock dating: an example from the African Restionaceae. Mol. Phylogenet. Evol. 35:569–582.
Litsios G., Salamin N. 2012. Effects of phylogenetic signal on ancestral state reconstruction. Syst. Biol. 61:533–538.
Lomolino M.V., Riddle B.R., Whittaker R.J., Brown J. H. 2010. Biogeography (4th edition). Sunderland, MA: Sinauer Associates.
Maddison W.P., Midford P.E., Otto S.P. 2007. Estimating a binary character's effect on speciation and extinction. Syst. Biol. 56: 701–710.
Magallón S., Sanderson M.J. 2001. Absolute diversification rates in angiosperm clades. Evolution 55:1762–1780.
Maguire K.C., Stigall A.L. 2009. Using ecological niche modeling for quantitative biogeographic analysis: a case study of Miocene and Pliocene Equinae in the Great Plains. Paleobiology 35:587–611.
Mao K., Milne R.I., Zhang L., Peng Y., Liu J., Thomas P., Mill R.R., Renner S.S. 2012. Distribution of living Cupressaceae reflects the breakup of Pangea. Proc. Natl Acad. Sci. U. S. A. 109:7793–7798.
Markwick P.J. 2007. The palaeogeographic and palaeoclimatic significance of climate proxies for data-model comparisons in deep-time prspectives on climate change. In: Williams M., Haywood A.M., Gregory F.J., Schmidt D.N., editors. Marrying the signal from computer models and biological proxies. London: The Geological Society, pp. 251–312.
Meseguer A.S., Aldasoro J.J., Sanmartin I. 2013. Bayesian inference of phylogeny, morphology and range evolution reveals a complex evolutionary history in St. John's wort (*Hypericum*). Mol. Phylogenet. Evol. 67:379–403.
Meseguer A.S., Sanmartín I. 2012. Paleobiology of the genus *Hypericum* (Hypericaceae): a survey of the fossil record and its palaeogeographic implications. An. Jard. Bot. Madr. 69:97–106.
Metcalf J.L., Prost S., Nogués-Bravo D., DeChaine E.G., Anderson C., Batra P., Araújo M.B., Cooper A., Guralnick R.P. 2014. Integrating multiple lines of evidence into historical biogeography hypothesis testing: a Bison bison case study. Proc. R. Soc. B Biol. Sci. 281:20132782.
Mildenhall D.C. 2006. *Hypericum* pollen determines the presence of burglars at the scene of a crime: an example of forensic palynology. Forensic Sci. Int. 163:231–235.
Nauheimer L., Metzler D., Renner S. 2012. Global history of the ancient monocot family Araceae inferred with models. New Phytol. 195:938–950.
Nogués-Bravo D., Rodríguez J., Hortal J., Batra P., Araújo M.B. 2008. Climate change, Humans, and the extinction of the Woolly Mammoth. PLoS Biol. 6:e79.
Nürk N.M., Madriñán S., Carine M.A., Chase M.W., Blattner F.R. 2013a. Molecular phylogenetics and morphological evolution of St. John's wort (*Hypericum*; Hypericaceae). Mol. Phylogenet. Evol. 66:1–16.

Nürk N.M., Scheriau C., Madriñán S. 2013b. Explosive radiation in high Andean *Hypericum*-rates of diversification among New World lineages. Front. Genet. 4:175.
Peterson A.T. 2011. Ecological niche conservatism: a time-structured review of evidence. J. Biogeogr. 38:817–827.
Phillips S.J., Anderson R.P., Schapire R.E. 2006. Maximum entropy modeling of species geographic distributions. Ecol. Model. 190:231–259.
Ree R.H., Moore B.R., Webb C.O., Donoghue M.J. 2005. A likelihood framework for inferring the evolution of geographic range on phylogenetic trees. Evolution 59:2299–2311.
Ree R.H., Smith S.A. 2008. Maximum likelihood inference of geographic range evolution by dispersal, local extinction, and cladogenesis. Syst. Biol. 57:4–14.
Robson N.K.B. 1981. Studies in the genus *Hypericum* L. (Guttiferae). 2. Characters of the genus. Bull. Br. Mus. Nat. Hist. (Bot.) 8:55–226.
Robson N.K.B. 2012. Studies in the genus *Hypericum* L. (Hypericaceae) 9. Addenda, corrigenda, keys, lists and general discussion. Phytotaxa 72:1–111.
Ronquist F., Sanmartín I. 2011. Phylogenetic methods in historical biogeography. Annu. Rev. Ecol. Evol. Syst. 42:441–464.
Ruhfel B.R. 2011. Systematics and biogeography of the clusioid clade (Malpighiales). Cambridge (MA): Harvard University.
Ruhfel B.R., Bittrich V., Bove C.P., Gustafsson M.H.G., Philbrick C.T., Rutishauser R., Xi Z., Davis C.C. 2011. Phylogeny of the clusioid clade (Malpighiales): evidence from the plastid and mitochondrial genomes. Am. J. Bot. 98:306–325.
Salzmann U., Haywood A.M., Lunt D.J., Valdes P.J., Hill D.J. 2008. A new global biome reconstruction and data-model comparison for the Middle Pliocene. Glob. Ecol. Biogeogr. 17:432–447.
Sanmartín I. 2012. Historical Biogeography: evolution in time and space. Evol. Educ. Outreach 5:555–568.
Sanmartín I., Enghoff H., Ronquist F. 2001. Patterns of animal dispersal, vicariance and diversification in the Holarctic. Biol. J. Linn. Soc. 73:345–390.
Schneck R., Micheels A., Mosbrugger V. 2012. Climate impact of high northern vegetation: Late Miocene and present. Int. J. Earth Sci. 101:323–338.
Scotese C.R. 2010. Point tracker. PALEOMAP Project. Arlington: University of Texas.
Senut B., Pickford M., Ségalen L. 2009. Neogene desertification of Africa. C. R. Geosci. 341:591–602.
Smith S.A. 2009. Taking into account phylogenetic and divergence-time uncertainty in a parametric biogeographical analysis of the Northern Hemisphere plant clade Caprifolieae. J. Biogeogr. 36:2324–2337.
Smith S.A., Donoghue M.J. 2010. Combining historical biogeography with niche modeling in the Caprifolium clade of *Lonicera* (Caprifoliaceae, Dipsacales). Syst. Biol. 59:322–341.
Stevens P.F. 2007. Hypericaceae. In: Kubitzki K., editor. The families and genera of vascular plants. Berlin: Springer, pp. 194–201.
Stigall A.L. 2012. Using ecological niche modelling to evaluate niche stability in deep time. J. Biogeogr. 39:772–781.
Stigall Rode A.L., Lieberman B.S. 2005. Using environmental niche modeling to study the Late Devonian biodiversity crisis. In: Over D.J., Morrow J.R., Wignall P.B., editors. Developments in Palaeontology and Stratigraphy. Elsevier, pp. 93–179.
Tiffney B.H. 1985a. The Eocene North Atlantic land bridge: its importance in Tertiary and modern phytogeography of the Northern Hemisphere. J. Arnold Arbor. 66:243–273.
Tiffney B.H. 1985b. Perspectives on the origin of the floristic similarity between eastern Asia and eastern North America. J. Arnold Arbor. 66:73–94.
Valencia-Barrera R., Comtois P., Fernandez-Gonzalez D. 2002. Bioclimatic indices as a tool in pollen forecasting. Int. J. Biometeorol. 46:171–175.
van der Hammen T. 1974. The Pleistocene changes of vegetation and climate in tropical South America. J. Biogeogr. 1:3–26.
Varela S., Lobo J.M., Hortal J. 2011. Using species distribution models in paleobiogeography: a matter of data, predictors and concepts. Palaeogeogr. Palaeoclimatol. Palaeoecol. 310:451–463.
Wallace A.R. 1876. The geographical distributions of animals. London: Macmillan.
Wiens J.J., Donoghue M.J. 2004. Historical biogeography, ecology and species richness. Trends Ecol. Evol. 19:639–644.
Wiens J.J., Harrison R. 2004. Speciation and ecology revisited: phylogenetic niche conservatism and the origin of species. Evolution 58:193–197.
Wijninga V.M., Kuhry P. 1990. A Pliocene flora from the subachoque valle (Cordillera Oriental, Colombia). Rev. Palaeobot. Palynol. 62:249–290.
Wolfe J.A. 1975. Some aspects of plant geography of the northern hemisphere during the Late cretaceous and Tertiary. Ann. Mo. Bot. Gard. 62:264–279.
Wolfe J.A. 1985. Distribution of major vegetational types during the Tertiary. The carbon cycle and atmospheric CO_2: natural variations archean to present. Proceedings of the Chapman Conference on Natural Variations in Carbon Dioxide and the Carbon Cycle, Tarpon Springs (FL), pp. 357–375.
Wood H.M., Matzke N.J., Gillespie R.G., Griswold C.E. 2012. Treating fossils as terminal taxa in divergence time estimation reveals ancient vicariance patterns in the Palpimanoid spiders. Syst. Biol. 62:264–284.
Yesson C., Culham A. 2006. Phyloclimatic modeling: combining phylogenetics and bioclimatic modeling. Syst. Biol. 55:785–802.
Zachos J.C., Dickens G.R., Zeebe R.E. 2008. An early Cenozoic perspective on greenhouse warming and carbon-cycle dynamics. Nature 451:279–283.